30 December 1994

ELSEVIER

Chemical Physics Letters 231 (1994) 551–560

CHEMICAL PHYSICS LETTERS

Time-resolved polarized fluorescence of the potential-sensitive dye RH421 in organic solvents and micelles

Nina V. Visser [a,*], Arie van Hoek [a], Antonie J.W.G. Visser [a], Ronald J. Clarke [b], Josef F. Holzwarth [b]

[a] *Department of Biochemistry, Agricultural University, Dreijenlaan 3, 6703 HA Wageningen, The Netherlands*
[b] *Department of Physical Chemistry, Fritz-Haber-Institut der Max-Planck-Gesellschaft, Faradayweg 4-6, D-14195 Berlin-Dahlem, Germany*

Received 29 August 1994

Abstract

Fluorescence lifetimes and time-resolved fluorescence anisotropy decays of the voltage-sensitive styrylpyridinium dye RH421 have been measured in various organic solvents and when bound to both anionic and cationic detergent micelles. At least two and often three exponential functions were necessary to fit the decay data. In organic solvents the form of the lifetime and anisotropy decays were dependent on the emission wavelength. In the red part of the emission spectrum an initial rise in fluorescence after the excitation pulse could be observed. This indicates the presence of a precursor–successor mechanism, in which a second fluorescent species is formed in an excited-state reaction. The initial fluorescence anisotropy (at zero time) was also higher for blue-detected emission than at the red edge, indicating a change in the angle of the emission transition moment of about nine degrees during the excited state lifetime. The results are discussed in terms of the formation of a fluorescent twisted intramolecular charge transfer state, occurring simultaneously with the relaxation of the surrounding solvent cage. The results in micellar systems suggest a distribution of dye over different sites within the micelle.

1. Introduction

Potential-sensitive fluorescent styryl dyes are presently being widely employed for the visualization of voltage transients in membrane preparations [1–3]. They have two main advantages over the use of microelectrodes. Firstly, they can be applied to the measurement of the membrane potential of any type of cell or cell organelle irrespective of their size. Secondly, they offer the possibility of recording voltage transients at different sites on a single cell or from many individual cells simultaneously at the molecular level. Therefore, they are of particular interest in the investigation of neuronal activity and neural networks.

Due to its high sensitivity RH421 (Fig. 1) is one of the most widely used styryl dyes. The mechanism

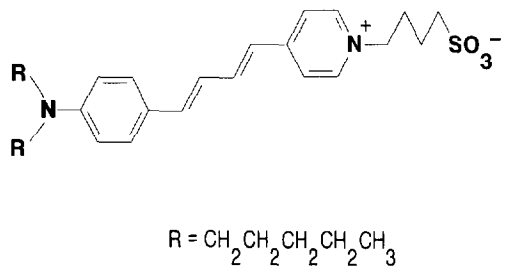

Fig. 1. Structure of RH421.

* Corresponding author. Telefax: 31-8370-84801.

SSDI 0009-2614(94)01276-8

by which a change in membrane potential is converted into a fluorescent signal from the dye is, however, still largely unknown. Several mechanisms have been proposed, including electrochromism, dye reorientation and the formation of a twisted internal charge transfer (TICT) state [4–6].

An important step towards a clarification of the voltage-sensitive mechanism is a complete understanding of the photophysics of the dye and how they are influenced by a change in its environment. In this Letter, therefore, we describe a study of the fluorescence kinetics and the fluorescence anisotropy kinetics of RH421 in various solvents of differing polarities and viscosities as well as in micellar systems.

2. Experimental

2.1. Materials

The dye N-(4-sulphobutyl)-4-(4-(*p*-dipentylaminophenyl)-butadienyl)-pyridinium inner salt (RH421) was obtained from Molecular Probes (Eugene, OR). It was kept as a 1.9 mM stock solution in ethanol at −20°C. Octanol, chloroform, ethanol and propylene glycol of best purity grade available were purchased from Merck (Darmstadt, Germany). Propylene glycol was distilled under reduced pressure. Solutions were made by adding a few microliters of RH421 to 1 ml organic solvent to have a final absorbance of 0.05 at 460 nm. Solutions were prepared fresh about 15 min prior to measurements. CTAC (hexadecyltrimethyl-ammonium chloride) was from Eastman Kodak (Rochester, NY) and STS (sodium tetradecyl sulfate) was obtained from Fluka (Buchs, Switzerland). Micelles were prepared by dissolving a pre-weighed amount of desired surfactant (10^{-3}–10^{-2} M final concentration) in buffer under vigorous stirring. One hour prior to measurements a few microliters RH421 from the ethanolic stock solution was added to 1 ml of solution in such a way that the molar ratio of dye to surfactant was 1:1000. The absorbance at 460 nm was in the range 0.05–0.10. All solutions were equilibrated at 30°C.

2.2. Methods

Polarized time-resolved fluorescence decay curves of RH421 under different solution conditions were acquired using a picosecond laser system in combination with time-correlated single-photon counting as described in detail elsewhere [7,8]. The excitation wavelength was 460 nm and the fluorescence was detected in three regions of the fluorescence spectrum. It was found that the emission spectra of RH421 in micellar solution were blue shifted and broadened as compared to the dye in homogeneous solution. For detection at the blue edge of the emission either 568.5 nm (RH421 in micelles) or 591.2 nm (RH421 in organic solvents) interference filters (bandwidth typically about 15 nm, Schott, Mainz, Germany) in combination with an OG515 cutoff filter (Schott) were used. As a reference compound for these emission wavelengths erythrosin B in water ($\tau = 80$ ps) was used [8]. For detection at the main emission band and at lower energies, the fluorescence was selected with OG515 and RG645 (Schott) cutoff filters. Red-edge detection was accomplished with the aid of either a RG695 (Schott) filter for RH421 in organic solvents or a RG715 (Schott) filter for RH421 in micelles and OG515 cutoff filters. For the central and red detection regions the instrumental response function was taken from the fluorescence of pinacyanol in ethanolic solution having an absorbance of 0.05 at 460 nm. The ultrashort decay time of this compound is about 10 ps [4]. The channel width of the multichannel analyzer amounted to 10 ps/channel and each decay curve was collected in 1024 channels. The temperature of the measurements was set at 30°C.

Data analysis was performed by the second generation global analysis software program described by Beechem et al. [9] and obtained from Globals Unlimited™ (Urbana, IL). First, the total fluorescence decay of individual experiments on one sample was analyzed in order to search for common decay parameters. The trial total fluorescence decay function was

$$S(t) = \sum_{i=1}^{n} \alpha_i \exp(-t/\tau_i) , \qquad (1)$$

in which α_i is the pre-exponential factor belonging to the lifetime component τ_i and n is the minimum number of lifetimes to have an acceptable fit to the data ($\chi^2 \approx 1.0$–1.5 and randomly scattered weighted residuals between experimental and fitted decay curves).

It was found that the 'blue' and sometime 'central'

decay curves require three components to have an acceptable fit to the experimental data. At the blue side of the fluorescence band an ultrashort decay component of unique value was found. Also two longer decay components were recovered. For RH421 in different organic solvents the longest decay component turned out to be common for all three decay curves and could be globally linked. At the red-edge of the fluorescence band a distinct rise in conjunction with a relatively long decay was seen, which could also sometimes be observed in the decay at the main fluorescence band but less pronounced. This rise term was usually linked over the two experiments selecting main-band and red-edge emission photons. After retrieving all fluorescence decay parameters these were fixed in a subsequent single time-resolved fluorescence anisotropy experiment in which the parallel and perpendicular decay curves were globally linked in a nonassociative fashion (for details see Ref. [10]). It turned out not to be feasible to globally link anisotropy parameters over the three emission-wavelength-dependent decay curves. It was sufficient for RH421 in organic solvents to fit the anisotropy decay to a single exponential function,

$$r(t)=\beta_1 \exp(-t/\phi_1)\,, \qquad (2)$$

in which ϕ_1 is the rotational correlation time and $\beta_1=r(0)$: the initial anisotropy at $t=0$.

A detailed error analysis at the 66% confidence level was carried out in order to estimate the reliable range of retrieved parameters. The procedure is described in Ref. [11].

3. Results

3.1. Polarized fluorescence decay parameters of RH421 in organic solvents

An example of the experimental fluorescence decays and associated analysis of RH421 in octanol has been presented in Fig. 2A. Usually three decay parameters were needed to fit the time-resolved fluorescence curves measured in the 'blue' and 'central' spectral regions. For the 'red' fluorescence profile two decay components were needed for a good fit: a rise and a decay term. In Fig. 2B we have also presented the three normalized time-dependent fluorescence

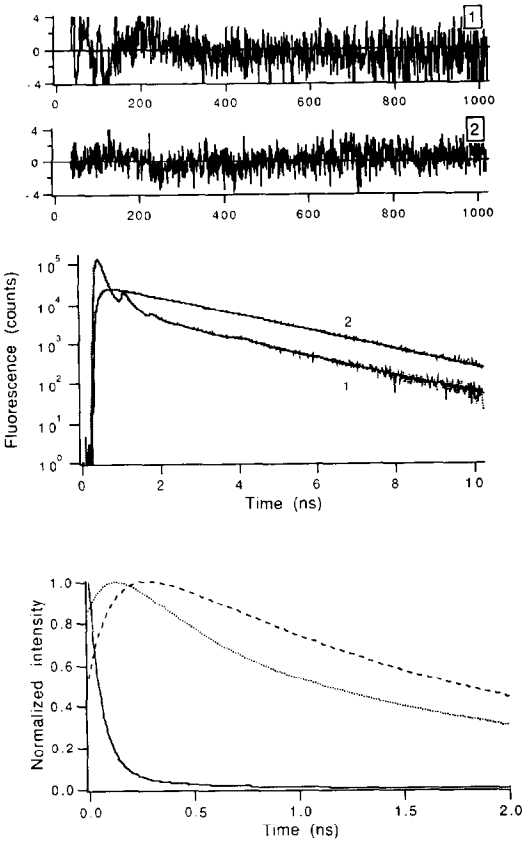

Fig. 2. (A) Fluorescence decay analyses of RH421 in octanol in the 'blue' (set of curves 1) and 'red' (set of curves 2) parts of the fluorescence spectrum. Sets 1 and 2 consist of two curves, namely experimental and fitted curves. The weighted residuals against channel number are shown at the top. $\chi^2=1.5$ for the 'blue' and $\chi^2=1.0$ for the 'red' part of the fluorescence spectrum. (B) Normalized (δ-impulse response) time-resolved fluorescence intensities of RH421 in octanol in the three spectral observation regions constructed from the parameters listed in Table 1. (——) Blue; (···) central; (– – –) red.

intensity profiles at the different emission wavelengths reconstructed from the decay parameters collected in Table 1. The rise which can be clearly seen in the red part of the emission and is still visible in the central part, is indicative of a precursor–successor mechanism in which a second species is created in an excited-state reaction involving a primary excited precursor [12]. It should then be noted that the pre-exponential factors and decay rates are functions of all rate constants of the system [9]. The decay rates are independent of the boundary conditions (for in-

Table 1
Fluorescence lifetimes and rotational correlation times of RH421 in various solvents and at different emission wavelengths

Wavelength [a]	α_1	τ_1 (ns)	α_2	τ_2 (ns)	α_3	τ_3 (ns)	β_1	ϕ_1 (ns)
chloroform								
blue	0.833	0.043 (0.039–0.048) [b]	0.037	0.6 (0.4–0.8) [b]	0.130	1.958 (1.956–1.980) [b]	0.38 (0.36–0.39) [b]	0.24 (0.21–0.25) [b]
central	−0.010	0.17 (0.12–0.19) [b]	0.055	0.6	0.955	1.958	0.35 (0.34–0.36) [b]	0.33 (0.30–0.34) [b]
red	−0.162	0.17	–	–	1.146	1.958	0.35 (0.34–0.36) [b]	0.32 (0.29–0.33) [b]
octanol								
blue	0.906	0.059	0.080	0.3	0.014	1.945	0.39	2.5
central	−0.646	0.12	0.646	0.3	0.853	1.945	0.36	3.2
red	−0.379	0.12	–	–	0.667	1.945	0.35	3.3
propylene glycol								
blue	0.971	0.024	0.019	0.4	0.010	1.393	0.40	6.8
central	0.292	0.12	0.066	0.4	0.642	1.393	0.38	9.4
red	−0.245	0.12	–	–	1.054	1.393	0.38	9.4
ethanol								
blue	0.844	0.019	0.132	0.2	0.024	1.019	0.37	0.38
central	0.136	0.15	–	–	0.864	1.019	0.36	0.53
red	−0.002	0.15	–	–	1.002	1.019	0.35	0.54

[a] Emission wavelength regions selected by the following filters: blue: 591.2 nm; central (+ red): RG645; red: RG695.
[b] Values in parentheses were from a detailed error analysis at 66% confidence interval.

stance, the relative light absorption of some species in the ground state at the excitation wavelength or the observation of some species in the excited state at a certain emission wavelength). The pre-exponential factors depend on both boundary conditions and decay rates.

All fluorescence decay parameters of RH421 in other solvents such as chloroform, propylene glycol and ethanol have been collected in Table 1. First it is apparent that in the blue part of the fluorescence spectrum the decay is dominated by an ultrashort fluorescence lifetime of tens of picoseconds (see pre-exponential factor α_1 in Table 1). The value seems to be related to the polarity of the solvent: the less polar the longer the lifetime. The longest fluorescence lifetime is more predominant in the central and red portions of the emission spectrum (see α_3 in Table 1). Also this lifetime is strongly dependent on the polarity: the more polar the shorter it becomes. The value of the risetime (see τ_1 in Table 1 for the central and red parts of the spectrum) does not seem to depend much on the type of solvent. The effect almost cancels in ethanol solution but is still visible owing to the high dynamic range of measurable intensities.

In Fig. 3A examples of the fluorescence anisotropy decay analysis have been presented for RH421 in octanol for the blue and red portions of the fluorescence spectrum. One correlation time was usually sufficient to obtain a good fit. It is immediately apparent that the initial anisotropy for the blue-detected emission is higher than the anisotropy (at zero time) at the red edge. If the initial portion of the time-dependent anisotropy at the red edge is expanded one notices that there is a slight rise in anisotropy almost together with the long-lived fluorescence (data not shown). The calculated anisotropy shows a slight misfit at the onset of anisotropy because the global program could not cope with the rise term in fluorescence (for this reason the residuals presented in Fig. 3A are not optimal). The initial anisotropy (at zero time) is, however, accurately determined. All fluorescence anisotropy decay parameters have been collected in Table 1. A striking result is that the correlation time at the blue edge of the emission is distinctly shorter than the ones measured at the central or red parts of the emission band. Because the decays are

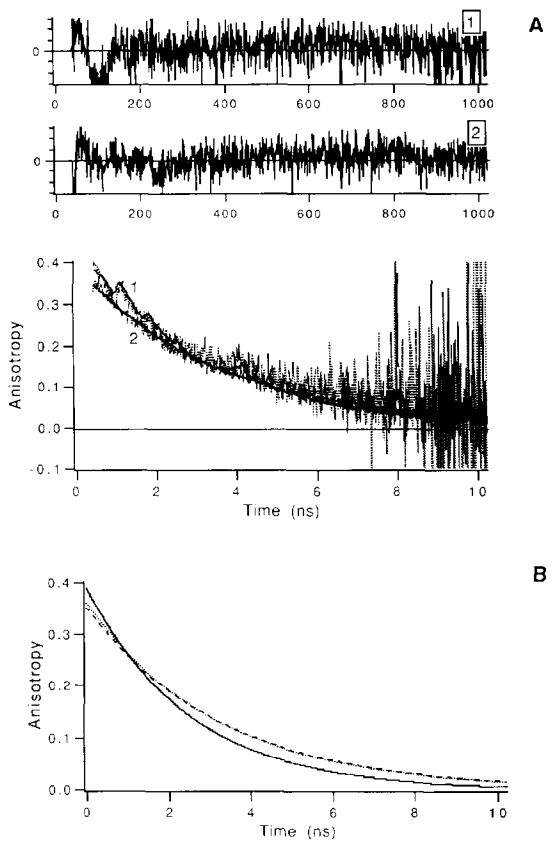

Fig. 3. (A) Fluorescence anisotropy decay analyses of RH421 in octanol in the 'blue' (set of curves 1) and 'red' (set of curves 2) parts of the fluorescence spectrum. Sets 1 and 2 were reconstructed from the individual polarized decay curves (parallel and perpendicular). Weighted residuals against channel number are shown at the top (details are given in Ref. [8]). $\chi^2 = 1.5$ for the 'blue' and $\chi^2 = 1.1$ for the 'red' part of the fluorescence spectrum. (B) Ideal (δ-impulse response) time-resolved fluorescence anisotropies of RH421 in octanol in the three spectral observation regions constructed from the parameters listed in Table 1. (——) Blue; (···) central; (– – –) red.

somewhat distorted in Fig. 3A, we have presented the ideal decays at the three observation wavelengths in Fig. 3B. These decays were constructed from the correlation times presented in Table 1; from Fig. 3B one can observe that the decays recorded in the central and red parts of the fluorescence spectrum are virtually identical. An inspection of Table 1 for the other data shows that both the latter effect and the faster anisotropy relaxation at the blue side of the emission are common for all solvents. Initial anisotropies close to the theoretical maximum value of 0.4 (for octanol or propylene glycol, see pre-exponential factor β in Table 1) strongly suggest that the transition dipole moment directions of absorption and emission are identical. At the blue side of the fluorescence spectrum one mainly observes the primary excited fluorophore which has a solvate (solute and solvent shell around it) configuration not very different from the ground state. However, the 'central' and 'red' emission photons originate from another solvate with a distinct change in emission transition moment direction and probably an increase in molecular volume, because the correlation time is distinctly longer. The values of the correlation times in different solvents scale well with the solvent viscosities. The slightly smaller initial anisotropies of RH421 in chloroform or ethanol arose from a tiny amount of slowly decaying residual anisotropy (amounting to about 0.01, data not shown). It is possible that the dye aggregates in these solvents which then becomes immediately visible owing to the high dynamic range of measurable anisotropy.

It is straightforward to calculate the relative angle δ_{BR} between emission transition moments of 'blue' and 'red' emitting RH421 species using the Lewschin formula [13] twice,

$$r_B(0) = \tfrac{3}{5}\cos^2\delta_B - \tfrac{1}{5}, \quad r_R(0) = \tfrac{3}{5}\cos^2\delta_R - \tfrac{1}{5},$$

$$\delta_{BR} = \delta_B - \delta_R . \qquad (3)$$

The relative angle δ_{BR} obtained from Eq. (3) was identical for RH421 in octanol and propylene glycol and amounted to 9°.

3.2. Polarized fluorescence decay characteristics of RH421 in micelles

When micelles are chosen with oppositely charged headgroups such as STS (negatively charged) and CTAC (positively charged) different charge effects on the spectroscopic properties can be expected. Upon incorporation of the dye in a micellar medium of low dielectric constant different Coulombic interaction between RH421 (which already possesses a charge separated ground state) and the surfactant heads will exist. Effects on the fluorescence decay of RH421 were observed. One characteristic feature was that it was virtually impossible to link all the fluorescence decay parameters over all three different observation

wavelengths. Only the longest decay component could be linked, mainly in the two decay experiments at longer wavelengths (central and red). Nonetheless, some trends can be distinguished. The fluorescence decay of RH421 is somewhat shorter in the case of the CTAC surfactant as reflected by the values of the fluorescence lifetime components collected in Table 2. This indicates that the local electric field has a distinct effect on the fluorescence quantum yield and lifetime. As a typical example the fluorescence decay and associated analysis of RH421 in STS micelles has been presented in Fig. 4A. Similarly, as in organic solvents, RH421 shows a rapid fluorescence lifetime component when the blue side of the emission band is observed, although its contribution is somewhat less than in the case of RH421 in organic solution. Only in the case of cationic micelles does the red-edge emission show a similar clear risetime as in homogeneous organic solution (Table 2). RH421 in anionic micelles does not show a clear growing-in of red emission, although a two- or three-component fit was needed. This is shown for the initial time-dependent fluorescence intensities given in Figs. 4B and 4C for RH421 in STS and CTAC micelles (curves generated from the parameters collected in Table 2). The same tendency was observed for RH421 in micelles made from other surfactants such as SDS (sodium decyl sulfate) and CDAC (dodecyltrimethyl ammonium chloride), but these results are not presented.

In Fig. 5A the fluorescence anisotropy decays and associated analysis of RH421 in STS micelles are shown. The results are in sharp contrast with those of the dye in organic solvents. The anisotropy detected at the blue side of the emission band decays considerably slower than that observed at the red edge of the fluorescence. At the blue edge the anisotropy decay is biexponential with a short subnanosecond component characteristic of internal probe motion independent of the rotation of the micelle as a whole, which is reflected by the much longer correlation time. The long correlation time is a good measure of the size of the micelles. Similarly, as observed for the dye in homogeneous solution the initial anisotropy is lower at the red side of the emission band. Following the procedure outlined in the preceding section we found that the angle between the emission transition moments averaged for the two micelles at $\delta_{BR}=9.5°$. The anisotropy decay at the red edge can be adequately described by a single correlation time. This emission-wavelength dependence of the anisotropy behaviour is general for all micelles, irrespective of charge and size (see results collected in Table 3 and the graphs depicted in Figs. 5B and 5C for RH421 in STS and in CTAC, respectively).

The polarized fluorescence results of RH421 in micelles may be interpreted as follows. The dye occupies different positions in the micellar interior. This implies that both fluorescence decay and fluorescence anisotropy decay arise from at least two microenvironments. The first may consist of the dye located close to the surfactant headgroup and this type of fluorophore mainly emits 'blue' photons. The ro-

Table 2
Fluorescence lifetimes of RH421 in micelles of STS (anionic) and CTAC (cationic) and at different emission wavelengths

Wavelength [a]	α_1	τ_1 (ns)	α_2	τ_2 (ns)	α_3	τ_3 (ns)
STS						
blue	0.660	0.047 (0.038–0.055) [b]	0.143	0.32 (0.27–0.40) [b]	0.196	1.25 (1.23–1.27) [b]
central	–	–	−0.366	0.87 (0.81–0.95) [b]	1.367	1.25 (1.23–1.27) [b]
red	–	–	−1.945	1.15 (0.79–1.2) [b]	2.945	1.25 (1.23–1.27) [b]
CTAC						
blue	0.802	0.044	0.136	0.29	0.062	0.86
central	–	–	0.371	0.59	0.629	1.04
red	–	–	−0.314	0.12	1.340	1.04

[a] Emission wavelength regions selected by the following filters: blue: 568.2 nm; central (+red): RG645; red: RG715.
[b] Values in parentheses were from a detailed error analysis at 66% confidence interval.

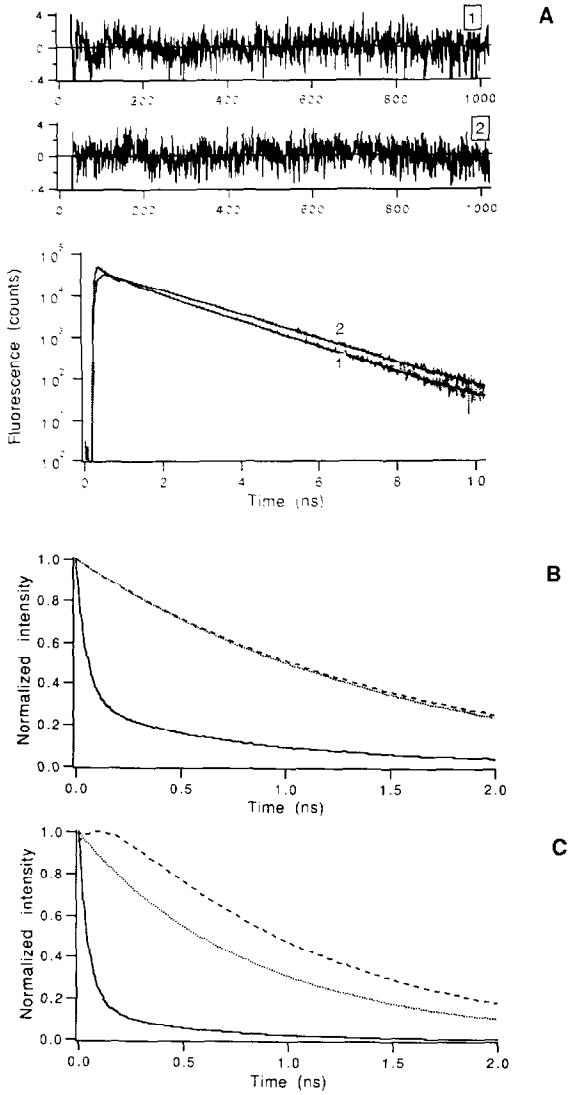

Fig. 4. (A) Fluorescence decay analyses of RH421 in STS (anionic) micelles in the 'blue' (set of curves 1) and 'red' (set of curves 2) parts of the fluorescence spectrum. Further details are as mentioned in the legend of Fig. 2. $\chi^2 = 1.1$ for the 'blue' and $\chi^2 = 1.1$ for the 'red' part of the fluorescence spectrum. (B), (C) Normalized (δ-impulse response) time-resolved fluorescence intensities of RH421 in STS (anionic) micelles (B) and in CTAC (cationic) micelles (C) in the three spectral observation regions constructed from the parameters listed in Table 2. (——) Blue; (···) central; (– – –) red.

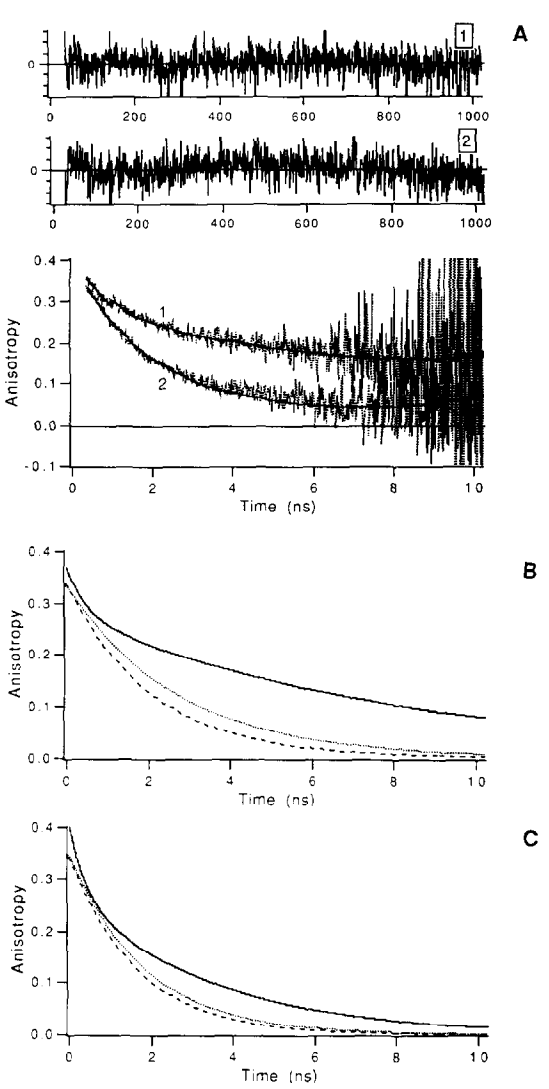

Fig. 5. (A) Fluorescence anisotropy decay analyses of RH421 in STS (anionic) micelles in the 'blue' (set of curves 1) and 'red' (set of curves 2) parts of the fluorescence spectrum. Further details are as mentioned in the legend of Fig. 3. $\chi^2 = 1.0$ for the 'blue' and $\chi^2 = 1.2$ for the 'red' part of the fluorescence spectrum. (B), (C) Ideal (δ-impulse response) time-resolved fluorescence anisotropies of RH421 in STS (anionic) micelles (B) and in CTAC (cationic) micelles (C) in the three spectral observation regions constructed from the parameters listed in Table 3. (——) Blue; (···) central; (– – –) red.

tational properties are similar to that found earlier for the dye octadecyl-rhodamine B in triton X100 micelles [14] with two rotational components describing fast internal and slower overall micellar rotation. The second micro-environment may originate from RH421 located in the more fluid interior

Table 3
Rotational correlation times of RH421 in micelles of STS (anionic) and CTAC (cationic) and at different emission wavelengths

Wavelength [a]	β_1	ϕ_1 (ns)	β_2	ϕ_2 (ns)
STS				
blue	0.09 (0.07–0.12) [b]	0.46 (0.24–0.82) [b]	0.28 (0.27–0.40) [b]	8.1 (6.4–12.6) [b]
central	–	–	0.334 (0.328–0.339) [b]	2.70 (2.62–2.90) [b]
red	–	–	0.337 (0.330–0.342) [b]	2.07 (1.98–2.16) [b]
CTAC				
blue	0.13	0.41	0.27	3.5
central	–	–	0.347	1.81
red	–	–	0.343	1.63

[a] Emission wavelength regions selected by the following filters: blue: 568.2 nm; central (+ red): RG645; red: RG715.
[b] Values in parentheses were from a detailed error analysis at 66% confidence interval.

of the micelle and this type of fluorophore preferably emits 'red' photons. The main evidence comes from the anisotropy results, indicating that the correlation time measured in the red part of the spectrum is too short to account for overall micellar motion. The fact that it turned out to be impossible to link common fluorescence decay parameters in the global analysis of the three emission-wavelength-dependent decays is indirect evidence that there are at least two fluorophore micro-environments with different decay parameters which probably do not interconvert on the timescale of the experiment.

4. Discussion

The photochemistry and photophysics of an aminostilbazolium dye of similar structure to RH421 have been extensively investigated by Ephardt and Fromherz [5]. These authors also provided a compilation of the available spectroscopic literature on this potential-sensitive probe. A reaction scheme has been proposed to explain the experimental results. This scheme consists of the following molecular states:

- ground state in trans conformation (T)
- ground state in cis conformation (C)
- a fluorescent state reached from the T-state (F)
- from the F-state two non-radiative excited states can be unidirectionally reached:
  - the twisted intramolecular charge transfer (TICT) state (I)
  - the state which is on the photoisomerization pathway (P).

From the excited P state the molecule can return nonradiatively to either T- or C-ground states. Reaching the P state involves a higher activation energy than reaching the I state. Since both I and P states are nonfluorescent this scheme would only yield monoexponential decays with a single fluorescent lifetime. This is not in agreement with the experiments described in this Letter.

The presence of another fluorescent species is proven by energy-dependent fluorescence intensity decays in which the growing-in of a certain species could be clearly observed in homogeneous solution and in CTAC micelles in the 'red' part of the emission spectrum. This indicates the presence of at least two emitting states: a precursor state whose rate of disappearance is faster than the rate of formation of the successor state (compare $1/\tau_1$ values for blue and red emissions in Table 1). It is reasonable to assign the precursor to the F state which could have other radiationless pathways because its fluorescence lifetime is shorter. An estimate of the rate of formation of the successor state (I) can be done by taking the reciprocal of the lifetime of the growing-in phase provided that there is no back reaction from the I to the F state. From $1/\tau_1$ values in Table 1 this rate constant then varies between 8.3 ns^{-1} for propylene glycol or octanol to 5.9 ns^{-1} for chloroform. Further evidence came from anisotropy decay data which were shown to depend on the emission energy as well.

It is therefore tempting to assign the 'second' species to a fluorescent TICT state in which the emission transition moment changes over 9° degrees with respect to the primary excited F state. In homogeneous solution the molecule in the TICT state is characterized by a distinctly larger molecular volume since it rotates more slowly. Because of the larger dipole moment in the TICT state the polarizability of solvent molecules is enhanced and this may result in the attachment of an outer solvent layer which makes the net volume of the solvate larger. In the micellar systems it seems that the dye is distributed over at least two regions of the micellear interior. RH421 in these compartments has different fluorescence relaxation characteristics which can be distinguished by selecting different energies of the fluorescence transition.

Rettig and co-workers [15,16] also proposed a fluorescent TICT state for dyes of similar structure. From that work it was not possible to exclude solvent relaxation as a contribution to the time-resolved shift of the emission spectrum. In the case of RH421 it is also possible that the reorganization of the surrounding solvent cage is occurring on the same timescale as the TICT state formation. Declémy and co-workers [17] have reported a relaxation time of 90 ps at 20°C for the reorganization of butanol around a model compound for pure solvent cage effects. This is of the same order of magnitude as the relaxation time for the 'growing-in' phase reported here.

Finally, the relevance of the results for the voltage sensitivity of the dye should be discussed. Ephardt and Fromherz [5] proposed two mechanisms which could lead to a change in quantum yield of fluorescence: (1) a direct yield mechanism, in which the electric field interacts with the redistribution of charge in the dye after excitation, so that the rate of formation of the TICT state is changed, and (2) an indirect yield mechanism, in which the electric field causes a dislocation of the dye in the lipid membrane and as a consequence a change in environment, i.e. a change in polarity or viscosity, resulting in a change in the rate of formation of the TICT state. Both mechanisms would be expected to produce a significant change in quantum yield, if the efficiencies of radiationless deactivation of the precursor and successor states are very different. Ephardt and Fromherz [5] proposed that the TICT state is nonradiative, whereas the initially reached excited state is fluorescent. A change in the rate of formation of the TICT state would in this case result in a significant change in the overall quantum yield. For RH421, however, the situation is very different. Both the precursor and successor species are fluorescent, although the fluorescence lifetime of the successor species is longer than that of the precursor. Under these circumstances the effect of an applied electric field on the overall quantum yield would not be expected to be as significant. In order to clarify this point experiments in synthetic and natural membranes in the presence and absence of an electric field are in progress.

Acknowledgement

One of us (NVV) was supported by a fellowship from the Fritz-Haber-Institut der Max-Planck-Gesellschaft. RJC acknowledges with gratitude financial support from the Deutsche Forschungsgemeinschaft.

References

[1] J.C. Smith, Biochim. Biophys. Acta 1016 (1990) 1.
[2] A. Grinvald, R.D. Frostig, E. Lieke and R. Hildesheim, Physiol. Rev. 68 (1988) 1285.
[3] L.M. Loew, ed., Spectroscopic membrane probes (CRC Press, Boca Raton, 1988).
[4] A. Zouni, R.J. Clarke, A.J.W.G. Visser, N.V. Visser and J.F. Holzwarth, Biochim. Biophys. Acta 1153 (1993) 203.
[5] H. Ephardt and P. Fromherz, J. Phys. Chem. 93 (1989) 7717.
[6] P. Fromherz and A. Lambacher, Biochim. Biophys. Acta 1068 (1991) 149.
[7] A. van Hoek and A.J.W.G. Visser, Proc. SPIE 1640 (1992) 325.
[8] P.I.H. Bastiaens, A. van Hoek, J.A.E. Benen, J.C. Brochon and A.J.W.G. Visser, Biophys. J. 63 (1992) 839.
[9] J.M. Beechem, E. Gratton, M. Ameloot, J.R. Knutson and L. Brand, in: Topics in fluorescence spectroscopy, Vol. 2, ed. J.R. Lakowicz (Plenum Press, New York, 1992) p. 241.
[10] K. Vos, A. van Hoek and A.J.W.G. Visser, Eur. J. Biochem. 165 (1987) 55.
[11] J.M. Beechem and E. Gratton, Proc. SPIE 909 (1988) 70.
[12] A.J. Kungl, G. Landl, A.J.W.G. Visser, M. Breitenbach and H.F. Kauffman, J. Fluorescence 2 (1992) 63.
[13] G. Weber, in: Fluorescence techniques in cell biology, eds. A.A. Thaer and M. Sernetz (Springer, Berlin, 1973) p. 5.
[14] A.J.W.G. Visser, K. Vos, A. van Hoek and J.S. Santema, J. Phys. Chem. 92 (1988) 759.

[15] R. Lapouyade, K. Czeschka, W. Majenz, W. Rettig, E. Gilabert and C. Rullière, J. Phys. Chem. 96 (1992) 9643.
[16] W. Rettig, W. Majenz, R. Lapouyade and M. Vogel, J. Photochem. Photobiol. A 65 (1992) 95.
[17] A. Declémy, C. Rullière and Ph. Kottis, Chem. Phys. Letters 133 (1987) 448.